ELSEVIER

Research Focus

Three-dimensional analysis of plant structure using high-resolution X-ray computed tomography

Wolfgang H. Stuppy[1], Jessica A. Maisano[2], Matthew W. Colbert[2], Paula J. Rudall[3] and Timothy B. Rowe[2]

[1]Royal Botanic Gardens, Kew, Seed Conservation Department, Wakehurst Place, Ardingly, West Sussex RH7 6TN, UK
[2]High-Resolution X-ray CT Facility, Jackson School of Geosciences, The University of Texas at Austin, C1100, Austin, TX 78712, USA
[3]Royal Botanic Gardens, Kew, Richmond, Surrey TW9 3AB, UK

High-resolution X-ray computed tomography (HRCT) is a non-invasive approach to 3D visualization and quantification of biological structure. The data, based on differential X-ray attenuation, are analogous to those otherwise obtainable only by serial sectioning. Requiring no fixing, sectioning or staining, HRCT produces a 3D digital map of the specimen that allows measurements and visualizations, including arbitrarily oriented sections. In spite of its application throughout the natural sciences, HRCT has yet to be applied in extant plant structural research.

Computed tomography (CT) originated in 1971 as a medical diagnostic tool. Conventional medical CT scanners are designed for human-sized objects and densities and therefore use non-lethal X-ray energies (~75 kV), and thus cannot resolve slices less than 1–2 mm thick [1]. Because high-resolution X-ray CT (HRCT) uses more sophisticated detector arrays and more powerful X-ray sources (up to 420 kV [2]) than medical CT does, its spatial resolution is nearly 100-fold greater (maximum resolution a few tens of microns [μm] [2]). It also has greater penetration, density discrimination and flexibility in imaging, enabling new materials and size classes to be scientifically observed. For example, HRCT has been used to address a wide range of questions in the earth sciences (e.g. [1,3]), palaeontology (e.g. [4–6]) and zoology (e.g. [7,8]).

Palaeobotanists have not exploited HRCT technology for their research, although a brief investigation by Milena Pika-Biolzi *et al.* [9] demonstrated its considerable potential for this field. They were able to distinguish pith, xylem, cortex, vascular bundles, leaf bases, seeds and ovuliferous scales in the fossilized trunk of a species of *Cycadeoidea* from the late Jurassic in the UK and in a petrified cone of *Araucaria mirabilis* from the Jurassic Cerro Cuadraro Petrified Forest in Patagonia (Argentina). For recent plant material, the use of HRCT has been limited to investigations of the morphological development and spatial distribution of root systems *in situ* [10,11]. We present here the first documentation of the potential application of HRCT to a wide range of extant plant materials and briefly review the results in the context of other non-invasive imaging techniques.

Corresponding author: Wolfgang H. Stuppy (w.stuppy@rbgkew.org.uk).

Applicability of HRCT to plant material

Six common, commercially available samples were selected for HRCT examination without any special treatment before scanning. Emphasis was placed on testing plant parts that show contrasting tissue densities; that is, tissues with different X-ray attenuation properties (especially soft versus hard tissues). 'Hard' objects examined with low water content and a variety of tissue densities included the fruit of a South American palm ('Coco Do Vaqueiro', *Syagrus flexuosa*, Arecaceae) and a piece of English oak wood (*Quercus robur*, Fagaceae). Fresh and fully turgid 'soft' objects examined with high water content and low tissue-density differences included a pineapple (*Ananas comosus*, Bromeliaceae), a tulip flower (*Tulipa* hybr., Liliaceae) and an inflorescence of *Leucospermum tottum* (Proteaceae). All specimens were scanned at the HRCT Facility at The University of Texas at Austin (USA).

In large plant parts with little or no tissue-density heterogeneity, such as in the weakly lignified pineapple fruit, tulip flower and *Leucospermum tottum* inflorescence, HRCT detected little contrast beyond that between void spaces and tissue (Fig. 1a). Yet this method produces accurate 3D visualizations of the external morphology of these 'soft' objects (Fig. 1b,c), the volumes and surface areas of which are then easily quantified.

Differences in X-ray attenuation in plant tissues and organs depend primarily upon the thickness and consistency of cell walls and cell contents. Thus, for differentiating internal structures, the best results were obtained from samples that contained a broad range of tissues of different densities, such as wood, fruits and seeds.

In oak wood, even at relatively low resolution (~50 μm interpixel distance in scan plane), periderm, phloem and xylem tissues are readily distinguished by their differences in X-ray attenuation (Fig. 2a). Even further discrimination between tissue types is possible within the secondary xylem itself; for example, axial and radial parenchyma (including narrow vessels) and fibres. Individual cells are not discernible, with the exception of the wide (up to ~400 μm) earlywood vessels at the beginning of each growth ring that appear as black holes in the scan. Infillings of these void spaces can be rendered in 3D (Fig. 2b) to study the connectivity and carrying capacity of earlywood vessels in different types of wood.

The potential of HRCT for examination of complex

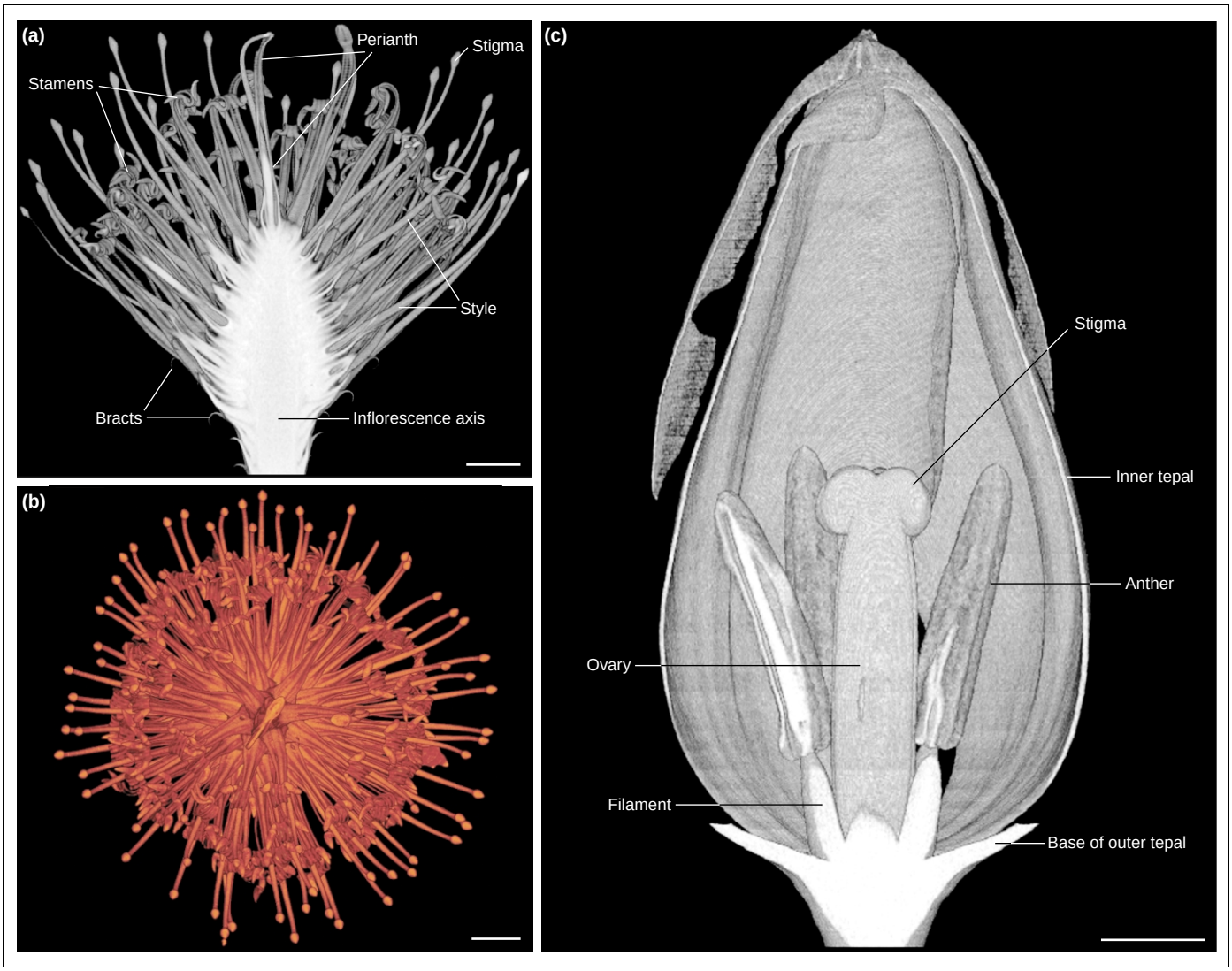

Fig. 1. (a) Three-dimensional cutaway reconstruction of the inflorescence of *Leucospermum tottum*. The inflorescence consists of numerous bisexual zygomorphic flowers. Each individual flower is subtended by a bract and has a style, four stamens and a cylindrical perianth. The perianth is longitudinally split by the lengthening style into a free lower segment with one stamen that becomes coiled after anthesis and an upper portion that is separated at the tip into three distinct lobes, each carrying a stamen. The sessile ovary at the base of the rigid style is too small to distinguish. Scale bar = 10 mm. (b) Three-dimensional false-coloured rendering of the apical aspect of the same inflorescence. Scale bar = 10 mm. (c) Three-dimensional cutaway reconstruction of the flower of *Tulipa* hybr. Although high-resolution X-ray computed tomography (HRCT) could detect little contrast beyond that between void spaces and tissue, it still provides an exact 3D image of the external morphology (the outer three tepals of the flower were digitally removed). Scale bar = 5 mm.

organs such as fruits and seeds is illustrated by the 3D reconstruction of the external and internal morphology of the fruit of *Syagrus flexuosa* (Fig. 3). There are sufficient differences in X-ray attenuation to enable the protective layers to be easily distinguished from the endosperm and embryo. The thickened and lignified cell walls of the mesocarpic fibres (i.e. the bristle-like hairs on the outside of the fruit; the smooth exocarp has been removed) and the hard endocarp (with less dense fibrovascular bundles) are responsible for the relatively strong X-ray attenuation. The endosperm appears to be less radio-opaque than the embryo is, probably because of the larger average cell size in the endosperm. Furthermore, significant morphological details are visible, such as the three pores at the base of the fruit, which represent openings in the hard endocarp (one per carpel) and the two aborted ovules in the endocarp.

Analogous methods for 3D visualizations

Visualization of 3D objects provided by HRCT is most comparable to that derived from nuclear magnetic resonance (NMR) imaging. With slightly greater resolution (typically 10 μm [12]), NMR can supply non-invasive 3D visualizations of a wide variety of plant structures [12–15]. In NMR, the water content of the objects examined is a crucial factor in determining pixel intensities. As a result, NMR allows a unique view of a variety of plant physiological processes, including water movement through vascular tissues *in vivo* [16,17]. However, HRCT is more suitable for 'dry' objects, such as dried plant parts (e.g. herbarium or wood specimens), dry fruits and seeds and fossilized material because it can penetrate denser materials and depends on overall density contrast rather than water content. HRCT cannot be used *in vivo* because the X-rays it uses are lethal.

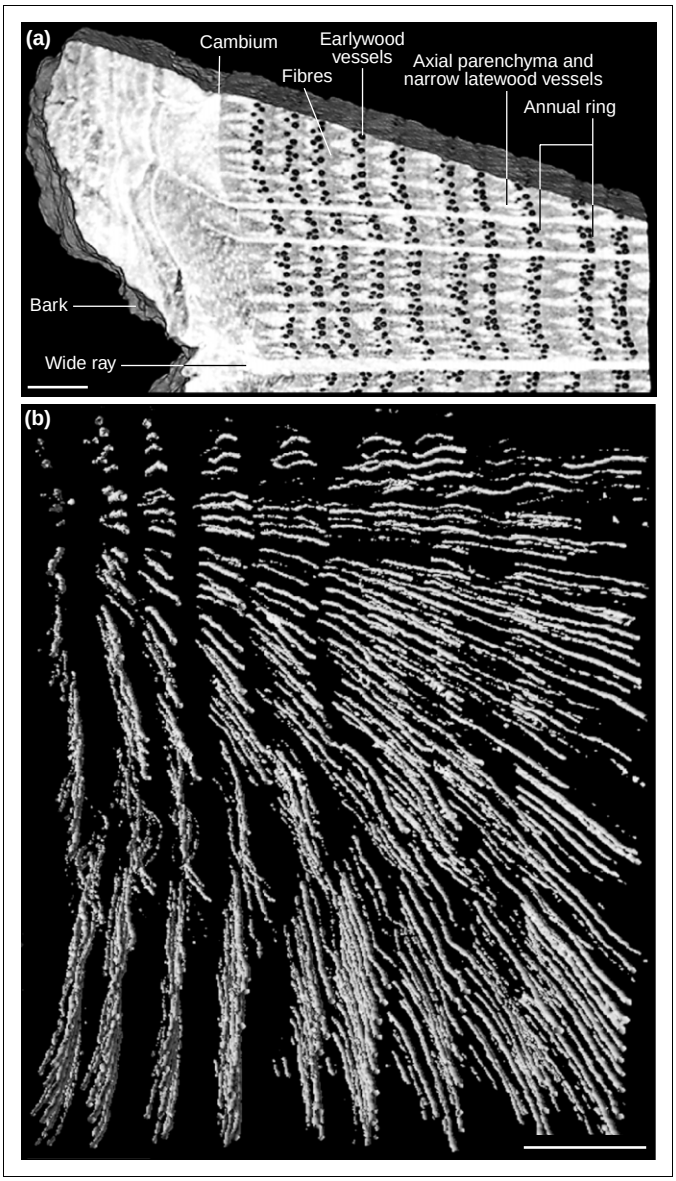

Fig. 2. (a) High-resolution X-ray computed tomography (HRCT) image showing a cross section of English oak wood (*Quercus robur*). Differences in X-ray attenuation allow clear distinction between bark (periderm and phloem) and wood (secondary xylem). In the wood, earlywood vessels (~400 μm in diameter) at the beginning of each growth ring appear as black holes, but other individual cells cannot be seen. Fibres are grey, and axial parenchyma and narrow latewood vessels are white, as are wide multiseriate rays that run radially from the phloem through the xylem. Cambium cannot be seen at this magnification, but its position between phloem and xylem is implied. (b) Three-dimensional reconstruction of infillings of the earlywood vessels showing their distribution and connectivity throughout the specimen volume. Scale bar = 5 mm.

Three-dimensional visualizations can also be achieved through confocal laser scanning microscopy (CLSM) [18,19], optical coherence microscopy (OCM) [20] and electron tomography (ET, using a transmission electron microscope) [21]. These methods currently yield higher resolution than HRCT does (reaching 2.5–5.0 nm for ET) and are therefore suitable for examination of structural composition and organization of cellular components, even at the macromolecular level (with ET). However, in contrast with HRCT and NMR, objects to be examined with CSLM, OCM and ET must be relatively thin and transparent or at least semi-transparent (e.g. OCM can penetrate up to 1 mm in living tissue [20]); these methods are therefore relatively restrictive in their application (Table 1).

Potential applications and future prospects of HRCT

HRCT has the potential to open new avenues for the qualitative and quantitative examination of the external and internal morphology and histology of plants. One of the main benefits of this novel technology is its non-invasiveness, which is particularly crucial for specimens that are too precious to study destructively, such as type specimens and rare fossils. The other main benefit of HRCT is its digital output, which permits graphic 3D visualizations as well as accurate and reproducible quantitative measurements. Using HRCT, more samples can be examined in greater detail and in much less time than can be with serial sectioning. Moreover, the non-invasive nature of the method allows not only the study of longitudinal and transverse sections, but also views from any arbitrary angle and perspective, using the same specimen.

Apart from being the only option in cases where sample size or other factors (e.g. consistency or rarity) do not allow for invasive serial sectioning (except for NMR in the case of relatively moist specimens), examination of complex organs, such as fruits and seeds or branching patterns of vascular systems, could benefit greatly from HRCT. Because industrial scanners can image large specimens (for example, the machine at the University of Texas at Austin can scan image specimens up to 50 cm in diameter and 75 cm in height), complex branching patterns of vascular systems and nodal anatomy could be investigated quickly and in detail in relatively large stem or root sections and even in whole plants. For example, investigations of vascular architecture in palms previously were carried out via the application of first film, then video

Table 1. Comparison of the major non-invasive 3D visualization technologies

Method	Strength	Weakness
HRCT	Objects can be large, dense and opaque	Contrasting densities crucial in determining pixel intensities
	Not dependent on water content	Lethal X-ray intensity does not permit developmental studies
	No sample preparation required	
NMR	Objects can be large and opaque	Water content crucial in determining pixel intensities
	Repeated exposure possible for *in vivo* (e.g. developmental) observations	
ET, CLSM, OCM	Higher resolution than HRCT and NMR	Objects must be small, thin and transparent or at least semi-transparent

Abbreviations: CSLM, confocal laser scanning microscopy; ET, electron tomography (using a transmission electron microscope); HRCT, high resolution X-ray computed tomography; NMR, nuclear magnetic resonance imaging; OCM, optical coherence microscopy.

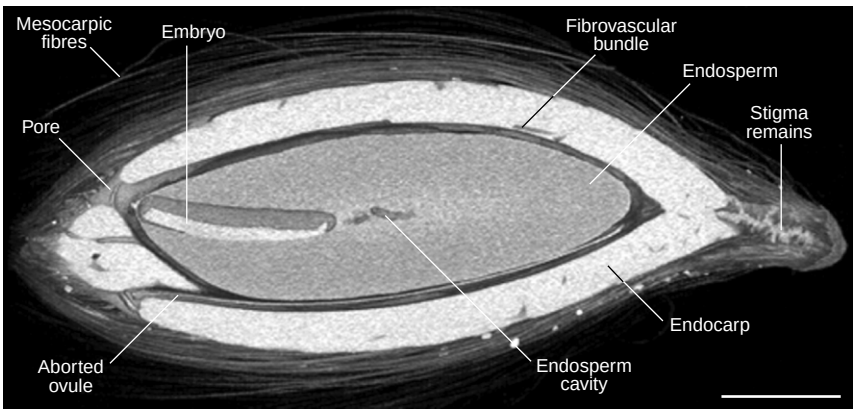

Fig. 3. Three-dimensional cutaway reconstruction of the fruit of the South American palm 'Coco Do Vaqueiro' (*Syagrus flexuosa*). High-resolution X-ray computed tomography (HRCT) clearly distinguishes all morphologically relevant parts and organs such as the peripheral meoscarpic fibres, endocarp with fibrovascular bundles and endosperm with embryo. Other significant morphological details revealed include a central cavity in the endosperm, one of the three pores at the base of the fruit, which represent openings in the hard endocarp, and one of the two aborted ovules. Scale bar = 5 mm.

recording of sequential images taken from serial sections of stems [22–24]. Apart from the compelling 3D visualizations, HRCT would generate an incomparably larger amount of (digital) data that would allow accurate dimensional and volumetric measurements. However, repeated exposure of live samples is not feasible with HRCT because of the intensity of the X-rays.

The resolution of HRCT technology is rapidly improving, and might soon allow detailed examination at the cellular level. Another possible application of HRCT in plant structural research would be non-invasive examination of the structure and physical qualities of secondary xylem; for example, in assessments of the biomechanical properties of different woods.

Finally, HRCT datasets can be transformed into surface models for hardcopy rendering by rapid prototyping machines. These reconstructions can be 'printed' at any scale by any of nearly 200 different mechanical devices and thereby serve as accurate botanical models. The files used to generate these printouts, along with other digital HRCT data and visualizations, are easily disseminated via the Internet. Thus, HRCT can be used not only to provide access to the detailed internal anatomy of a variety of recent plant materials but also to make that anatomy readily available to the worldwide scientific community.

The HRCT scans and resulting imagery described above can be viewed at the Digital Morphology Library (www.digimorph.org).

Acknowledgements

HRCT scanning and image processing were funded by a National Science Foundation Digital Libraries Initiative grant (IIS-9874781) to T.B.R. We gratefully acknowledge financial support from the Millennium Commission, the Wellcome Trust and Orange plc. We also thank Peter Crane for first suggesting this project, John Dickie, John Dransfield and Peter Gasson, Royal Botanic Gardens, Kew, for their help with the interpretation of the X-ray imagery and John Rourke, Kirstenbosch Research Centre, for the identification of the *Leucospermum* specimen. The fruits of *Syagrus flexuosa* were kindly provided by Christopher Wood, Royal Botanic Gardens, Kew.

References

1 Rowe, T. *et al.* (1997) High-resolution computed tomography: a breakthrough technology for earth scientists. *Geotimes* 1, 23–27
2 Denison, C. *et al.* (1997) Three-dimensional quantitative textural analysis of metamorphic rocks using high-resolution computed X-ray tomography. Part I. Methods and techniques. *J. Metamorph. Geol.* 15, 29–44
3 Ketcham, R.A. and Carlson, W.D. (2001) Acquisition, optimization and interpretation of X-ray computed tomography imagery: applications in the geosciences. *Comput. Geosci.* 27, 381–400
4 Rowe, T. (1996) Coevolution of the mammalian middle ear and neocortex. *Science* 273, 651–654
5 Rowe, T. *et al.* (2001) The *Archaeoraptor* forgery. *Nature* 410, 539–540
6 Tykoski, R.S. *et al.* (2002) *Calsoyasuchus valliceps*, a new crocodyliform from the early Jurassic Kayenta Formation of Arizona. *J. Vertebr. Paleontol.* 22, 593–611
7 Maisey, J.G. (2001) Remarks on the inner ear of elasmobranchs and its interpretations from skeletal labyrinth morphology. *J. Morphol.* 250, 236–264
8 Maisano, J.A. *et al.* (2002) The osteoderms and palpebral in *Lanthanotus borneensis* (Squamata: Anguimorpha). *J. Herpetol.* 36, 678–682
9 Pika-Biolzi, M. *et al.* (2000) Industrial X-ray computed tomography applied to paleobotanical research. *Riv. Ital. Paleontol. Stratigrafia* 106, 369–377
10 Heeraman, D.A. *et al.* (1997) Three dimensional imaging of plant roots *in situ* with X-ray computed tomography. *Plant Soil* 189, 167–179
11 Pierret, A. *et al.* (1999) X-ray computed tomography to quantify tree rooting spatial distributions. *Geoderma* 90, 307–326
12 Köckenberger, W. (2001) Functional imaging of plants by magnetic resonance experiments. *Trends Plant Sci.* 6, 286–292
13 Connelly, A. *et al.* (1987) High-resolution imaging of plant tissues by NMR. *J. Exp. Bot.* 38, 1713–1723
14 Ishida, N. *et al.* (2000) The NMR microscope, a unique and promising tool for plant science. *Ann. Bot.* 86, 259–278
15 Glidewell, S.M. *et al.* (2002) NMR imaging as a tool for noninvasive taxonomy: comparison of female cones of two Podocarpaceae. *New Phytol.* 154, 197–207
16 MacFall, J.S. and Johnson, G.A. (1994) The architecture of plant vasculature and transport as seen with magnetic-resonance microscopy. *Can. J. Bot.* 72, 1561–1573
17 Köckenberger, W. *et al.* (1997) A non-invasive measurement of phloem and xylem water flow in castor bean seedlings by nuclear magnetic resonance microimaging. *Planta* 201, 53–63
18 Hepler, P.K. and Gunning, B.E.S. (1998) Confocal fluorescence microscopy of plant cells. *Protoplasma* 201, 121–157
19 Veraverbeke, E.A. *et al.* (2001) Nondestructive analysis of the wax layer of apple (*Malus domestica* Borkh.) by means of confocal laser scanning microscopy. *Planta* 213, 525–533
20 Hettinger, J.W. *et al.* (2000) Optical coherence microscopy: a

technology for rapid, *in vivo*, non-destructive visualisation of plants and plant cells. *Plant Physiol.* 123, 3–15
21 (1992) In *Electron Tomography: Three-dimensional imaging with the TEM* (Frank, J., ed.), Plenum Press
22 Zimmermann, M.H. and Tomlinson, P.B. (1967) Anatomy of the palm *Raphis excelsa*. 4. Vascular development in apex of vegetative aerial axis and rhizome. *J. Arnold Arbor. Harvard Univ.* 48, 122–142
23 Zimmermann, M.H. and Tomlinson, P.B. (1974) Vascular patterns in palm stems – variations of *Raphis* principle. *J. Arnold Arbor. Harvard Univ.* 55, 402–424
24 Tomlinson, P.B. *et al.* (2001) Stem-vascular architecture in the rattan palm *Calamus* (Arecaceae-Calamoideae-Galaminae). *Am. J. Bot.* 88, 797–809

1360-1385/02/$ - see front matter
PII: S1360-1385(02)00004-3

Vitamin E biosynthesis: biochemistry meets cell biology

Daniel Hofius and Uwe Sonnewald

Institut für Pflanzengenetik und Kulturpflanzenforschung (IPK), Corrensstrasse 3, D-06466 Gatersleben, Germany

Vitamin E is thought to be involved in many essential processes in plants, but no functional proof has been reported. To study vitamin E deficiency in plants, a high-throughput biochemical screen for vitamin E quantification in *Arabidopsis* mutants has been developed, which has led to the identification of *VTE1*-encoding tocopherol cyclase. Interestingly, the corresponding maize mutation, *sxd1*, causes plasmodesmata malfunction, suggesting a link between tocopherol cyclase and plasmodesmata function.

Tocopherols are an important class of lipid-soluble compounds with antioxidant activities that are synthesized only by plants and other photosynthetic microorganisms. All tocopherols are amphipathic molecules: the hydrophobic prenyl tail associates with membrane lipids and the polar chromanol head groups are exposed to the membrane surface. Four naturally occurring derivatives of tocopherols (α-, β-, γ- and δ-tocopherol) have been described that differ only in number and position of methyl substituents on the aromatic ring (Fig. 1). The composition and the content of the different tocopherol components in plant tissues varies considerably, ranging from the extremely low levels found in potato tubers to the high levels found in oil seeds. In addition, plant tissues might contain tocotrienol derivatives that differ from tocopherols only in the degree of saturation of their hydrophobic tails [1,2]. Among the tocopherols, α-tocopherol is the predominant form in photosynthetic tissues, and is mainly localized in plastids. The particular enrichment in chloroplast membranes is probably related to the ability of tocopherols to quench or to scavenge reactive oxygen species and lipid peroxy radicals by physical or chemical means. In this way, the photosynthetic apparatus can be protected from oxygen toxicity and lipid peroxidation. In non-photosynthetic tissues, γ-tocopherol frequently predominates and can be involved in the prevention of autoxidation of polyunsaturated fatty acids [2].

The various tocopherol and tocotrienol derivatives – commonly referred to as vitamin E – represent essential micronutrients for humans. α-Tocopherol in particular, has been reported to have beneficial effects on human health. A decreased risk of cardiovascular disease and certain cancers and retardation of several degenerative disease processes have been achieved when vitamin E supplements have been taken at therapeutic doses (100 to 1000 International Units, I.U.) [1,3]. However, these vitamin E levels are greatly in excess of the recommended daily allowance (~40 I.U.) and cannot be obtained from the average plant-derived diet. Therefore, much effort is currently aimed at identifying the genes involved in tocopherol biosynthesis to improve vitamin E levels in crop plants by metabolic engineering [4,5].

Tocopherol biosynthetic pathway

Tocopherol biosynthesis proceeds via the condensation of homogentisate, derived from the shikimate pathway, and phytyl pyrophosphate (phytyl-PP), derived from the non-mevalonate pathway, through the action of the homogentisate prenyltransferase (HPT). This yields 2-methyl-6-phytylplastoquinone, the first true tocopherol intermediate and common precursor of all tocopherols (Fig. 1). Subsequent ring cyclization and methylation reactions result in the formation of the four major tocopherol derivatives. It is probable that the formation of γ- and δ-tocopherol proceeds via a common cyclase. Similarly, the final methylation reaction resulting in α- and β-tocopherol, respectively, is expected to be catalysed by the same methyltransferase (γ-TMT).

The enzymatic steps of tocopherol biosynthesis were elucidated by biochemical means nearly 20 years ago, but the membrane association of the enzymes in the inner chloroplast envelope [6] has made purification and subsequent gene identification difficult. In recent years, genomics-based approaches have been applied for *Arabidopsis thaliana* and the cyanobacterium *Synechocystis* to identify genes of the tocopherol pathway. For instance, the γ-TMT gene was isolated from the putative 10-gene tocopherol biosynthetic operon in *Synechocystis* sp. PCC 6803, using bioinformatics and gene disruption experiments [7]. Overexpression of an *Arabidopsis* orthologue greatly

Corresponding author: Uwe Sonnewald (sonnewald@ipk-gatersleben.de).